

Characterization of Matrigel interfaces during defined human embryonic stem cell culture

Naomi T. Kohen

Department of Materials Science and Engineering, University of California at Berkeley, Berkeley, California 94720

Lauren E. Little

Department of Chemical Engineering, University of California at Berkeley, Berkeley, California 94720

Kevin E. Healy^{a)}

Department of Materials Science and Engineering and Department of Bioengineering, University of California at Berkeley, Berkeley, California 94720

(Received 2 October 2009; accepted 19 November 2009; published 14 January 2010)

Differences in attachment, proliferation, and differentiation were measured for human embryonic stem (hES) cells cultured on various substrata coated with Matrigel™, a blend of extracellular matrix proteins derived from murine tumor cells. The authors observed that hES cells attach and grow poorly on Matrigel adsorbed onto polystyrene, while they proliferate when exposed to Matrigel adsorbed onto glass or oxygen plasma treated polystyrene (e.g., “tissue culture” treated polystyrene). Furthermore, hES cells grown on the Matrigel-coated tissue culture polystyrene are less likely to differentiate than those grown on the Matrigel-coated glass. To assess the mechanism for these observations, they replicated the cell culture interface in a quartz crystal microbalance with dissipation monitoring. In addition, they used ellipsometry and scanning electron microscopy to determine the thickness and topography of Matrigel on the varying surfaces. Matrigel formed a viscoelastic multilayer with similar thickness on all three surfaces; however, the network structure was different, where the adsorbed proteins formed a globular network on polystyrene, and fibrillar networks on the hydrophilic substrates. Matrigel networks on glass were denser than on oxygen plasma treated polystyrene, suggesting that the density and structure of the Matrigel network affects stem cell differentiation, where a denser network promoted uncontrolled hES cell differentiation and did not maintain the self-renewal phenotype. © 2009 American Vacuum Society.

[DOI: 10.1116/1.3274061]

I. INTRODUCTION

Human embryonic stem (hES) cells have the potential to differentiate into all cell types in the adult body and hold great promise for regenerative medicine;^{1,2} however, large-scale expansion of undifferentiated hES cells remains a major challenge.³ Self-renewal, i.e., undifferentiated proliferation, of hES cells requires coculturing these cells with either mouse or human fibroblast cells (i.e., a feeder layer of cells).^{4–6} Culturing with mouse fibroblast cells increases the risk of zoonoses and the expression of foreign oligosaccharide residues acquired from the murine feeder cells and culture medium.⁷ Culturing with feeder layer cells, either human or murine, also poses significant disadvantages in reproducibility and scalability that greatly limit their clinical potential. More recently, several groups described methods to culture hES cells under chemically defined conditions (reviewed in Ref. 8).^{9–13} These systems use either animal or human-derived extracellular matrix (ECM) proteins adsorbed to the culture substrata and nonconditioned serum-free (NC-SF) media to support the undifferentiated state. Compared to the cell-based feeder systems, ECM proteins offer several

advantages, including reduced risk of pathogen transmission and relative ease of scale-up. The most exploited of these ECM analogs is Matrigel™, an extraction from Engelbreth–Holm–Swarm mouse sarcomas that contains not only basement membrane components (laminin, collagen IV, heparin sulfate proteoglycans and entactin) but also matrix degrading enzymes, their inhibitors, and numerous growth factors (see Table I for composition used in hES cell culture).¹⁵ However, the ECM proteins used in these culture systems are expensive, hard to produce in large enough quantities for widespread clinical use, exhibit lot to lot variability, introduce unwanted contaminants, and do not support self-renewal of some hES cell lines.^{4,5}

The derivation, self-renewal, and differentiation of hES cells within a completely synthetic environment would offer significant advantages and progress toward a source of clinically usable hES cells. However, replacing the complex ECM components that hES cells require with a synthetic matrix has been proven challenging, and Matrigel adsorbed in the cell culture surface in NC-SF media is still the best currently available method to culture hES cells, in spite of the aforementioned limitations. In this work, we sought to characterize the physical properties of adsorbed Matrigel to aid in understanding the mechanisms by which hES cells interact with this complex mixture of ECM proteins. Ulti-

^{a)}Author to whom correspondence should be addressed; electronic mail: kehealy@berkeley.edu

TABLE I. Matrigel™ (growth factor reduced) composition (Ref. 14).

Protein	Percentage (%)	Growth factor	Concentration
Laminin	61	bFGF	0–0.1 pg/ml
Collagen IV	30	EGF	<0.5 ng/ml
Entactin	7	IGF-1	5 ng/ml
Heparin sulfate proteoglycan (mainly perlecan)	Not available	PDGF	<5 pg/ml
		NGF	<0.2 ng/ml
		TGF- β	1.7 ng/ml

mately, we envisage using this knowledge to engineer precise synthetic culture environments to control human stem cell behavior.

Accordingly, we have observed that hES cells behave differently when they are grown on Matrigel adsorbed onto different surfaces, suggesting that the adsorption of Matrigel and its resulting physical-chemical properties may influence cell function. Three substrates have typically been used for mammalian cell culture platforms: borosilicate glass, polystyrene, and polystyrene treated with an oxygen plasma for tissue culture, i.e., tissue culture polystyrene (TCPS). Borosilicate glasses were the first platforms used for cell culture, but with the advent of easily and cheaply manufactured clear, high strength plastics, such as polystyrene, glass was replaced as the cell culture platform. Initially, one of the leading manufacturers of plastics for cell culture, coated glass onto plastic, as it was empirically recognized that a hydrophilic surface was necessary for optimal cell growth.¹⁶ Gas plasma treatments were subsequently developed to render polystyrene surfaces hydrophilic.¹⁷ As such, tissue culture polystyrene and glass are both hydrophilic and have similar wetting properties (water-in-air contact angle of TCPS $\leq 29^\circ$ and of glass $\leq 29^\circ$).^{18,19} Despite those similarities, hES cells behave differently when they are grown on Matrigel adsorbed onto each surface. In this work, the room temperature gelling of Matrigel was replicated inside a quartz crystal microbalance. Quartz crystals with functionalized surfaces (i.e., SiO₂, polystyrene, and oxygen plasma treated polystyrene) were used to monitor the adsorption dynamics and viscoelastic properties of Matrigel. Scanning electron microscopy and ellipsometry were used to observe the topography and thickness of the adsorbed Matrigel, respectively. We correlated measured properties with observed hES cell behavior and determined that ECM proteins in Matrigel adsorb as viscoelastic multilayer networks, they have distinct morphology and density based on the underlying substrate, and they either promote self-renewal or differentiation depending on the network structure.

II. METHODS AND MATERIALS

A. Reagents

All water used in this study was ultrapure ASTM type I reagent grade water (18.2 M Ω ·cm). All glassware was cleaned by immersion in 2% CONTRAD 70 (Decon Laboratories Inc. King of Prussia, PA) in water for at least 2 h.

Following thorough rinsing, the glassware was baked dry at 120 °C. Growth factor reduced Matrigel™ was obtained from BD Biosciences (Bedford, MA) (Table I). Matrigel at 2mg/ml was diluted into knockout Dulbecco's modified Eagle medium (KO-DMEM) (Invitrogen, Carlsbad, CA) in two steps. In the first step the Matrigel was diluted into 5 ml of KO-DMEM and mixed thoroughly with a pipette, with caution to avoid bubbles. In the second step, the diluted Matrigel was further diluted with 20 ml of KO-DMEM and thoroughly mixed with a pipette. Phosphate buffered saline (PBS) (Invitrogen) used was at pH 7.4 and it did not contain calcium chloride or magnesium chloride. Hellmanex (Hellma GmbH & Co. KG) was used at 2% concentration. Polystyrene, molecular weight of $\sim 200\,000$ with 1.05 polydispersity (Sigma-Aldrich) was diluted into HPLC grade toluene (Fisher Scientific) to form a 2 wt % solution for spin casting onto the substrates.

B. Matrigel adsorption studies

In this study, we replicated standard procedures for coating hES cell culture substrata with Matrigel. Matrigel was stored at -20°C until ready for use and was then diluted with KO-DMEM for stem cell culture.⁹ The diluted Matrigel (~ 0.067 mg/ml) was stored at 4°C in a liquid state. For cell culture, diluted Matrigel was pipetted onto the tissue culture surfaces and allowed to gel at room temperature for at least 30 min. Prior to cell seeding, the remaining liquid was removed with a pipette. Cells were then seeded and placed in an incubator at 37°C and 5% CO₂.

1. Surface modification

Gold coated and Si/SiO₂ coated AT-cut quartz crystals (Qsense Inc., Glen Burnie, MD) and Si and SiO₂ wafers (International Wafer Service, Inc., Colfax, CA) were sonicated in the following solvents for 15 min: water, acetone, hexane, acetone, and water. Crystals and wafers were then dried with nitrogen and exposed to an oxygen plasma at 0.5 Torr O₂ partial pressure and 75 W power for 5 min. The SiO₂ coated quartz crystals and SiO₂ wafers were not subjected to any further treatment prior to an adsorption experiment. To prepare the polystyrene surfaces, 2 ml of 2 wt % polystyrene in toluene was spun cast onto the topside of a quartz crystal (for QCM-D) or a Si wafer (for ellipsometry and scanning electron microscopy) with a Headway Research Spincaster (model PWM32). Toluene was dropped onto the

gold crystals/Si wafers, which were then spun at 2000 rpm for 1 min to evaporate the toluene. Subsequently, 2 ml of 2 wt % polystyrene solution was dropped onto the center of the topside of the gold crystals/Si wafers, which were then spun at 2000 rpm for 1 min. The backside of the gold crystals was cleaned with a toluene soaked *q*-tip (to ensure the backside electrode was not coated in polystyrene). The gold crystals/Si wafers were annealed at 110 °C for at least 24 h. A spectroscopic reflectivity based thin film thickness measuring system (Filmetrics F120, San Diego, CA) was used to collect a reflectance spectrum for the polystyrene film and determine its thickness as ~ 100 nm. After annealing, untreated polystyrene coated crystals were immediately introduced into the QCM-D chamber, and untreated polystyrene coated Si wafers were immediately coated with KO-DMEM diluted Matrigel for ellipsometry and scanning electron microscopy (SEM) studies. Some of the polystyrene coated samples were treated to mimic tissue culture polystyrene by exposure to an oxygen plasma at 0.5 Torr O₂ partial pressure and 75 W power for 30 s (Plasmod, Tegal Inc., Richmond CA). From the reflectance spectrum, it was determined that less than 15 nm of polystyrene was etched off of the crystal during this step. After treatment with oxygen plasma, the polystyrene coated crystals were immediately introduced into the QCM-D chamber and the oxygen plasma treated polystyrene coated Si wafers were immediately coated with KO-DMEM diluted Matrigel for ellipsometry and SEM studies.

2. Quartz crystal microbalance

A quartz crystal microbalance with dissipation monitoring QCM-D E4 (Q-Sense, Sweden) was used in this study and is described in detail elsewhere.²⁰ Briefly, alternating current is applied to the piezoelectric quartz crystal so that it oscillates in a shear mode at its resonant frequency. Only negative overtones can be excited electrically, and in the Q-sense system, the first, third, fifth, seventh, ninth, eleventh, and thirteenth overtones (designated as F1, F3, F5, F7, F9, F11, and F13, respectively) are excited sequentially by applying the associated voltage. The dampening factor, or the dissipation, which is defined as the inverse of the *Q* factor, is the energy dissipated per oscillation divided by the total energy stored in the system. When the driving power is turned off, the decay from each overtone is recorded yielding the absolute values of the frequency (F1, F5, F7, F9, F11, and F13) and dissipation of each overtone (D1, D3, D5, D7, D9, D11, and D13). In this experiment F1 and D1 were ignored as they were not reliable.^{20,21}

Frequency and dissipation values were recorded in air for all crystals. All liquids were allowed to reach room temperature before introduction into the QCM-D chamber, which was set to 25 °C. To obtain a base line, PBS was introduced into the chamber at a rate of 200 μ l/min and allowed to thermally equilibrate with the chamber. After ensuring a steady signal (drift less than 1 Hz/10 min on any normalized overtone), KO-DMEM diluted Matrigel was flowed through the chamber and allowed to adsorb onto the functionalized

quartz crystal (i.e., SiO₂, polystyrene, or oxygen plasma treated polystyrene). After the adsorption was complete, PBS was flowed through the chamber at 200 μ l/min until the signal was steady. Finally, the detergent Hellmanex was flowed through the chamber at 200 μ l/min. Three crystals were prepared and measured for each substrate type.

3. Ellipsometry

Matrigel film thickness on each substrate (i.e., SiO₂, polystyrene, and oxygen plasma treated polystyrene) was determined by ellipsometry (Sentech SE400, HeNe laser $\lambda = 632.8$ nm, angle of incidence $\phi = 70^\circ$). A drop of KO-DMEM diluted Matrigel sufficient to cover the entire surface was deposited on appropriately treated wafers (i.e., SiO₂ no treatment, polystyrene coating, polystyrene coating and subsequent oxygen plasma treatment). The Matrigel was left to gel for at least 30 min prior to ellipsometry measurements. Measurements employed the following refractive indices for each surface: $n_{\text{silicon}} = 3.874 - 0.016i$ (Ref. 22) for the silicon support, $n_{\text{silicon oxide}} = 1.457$,²² $n_{\text{polystyrene}} = 1.59$,²³ $n_{\text{Matrigel}} = 1.46$,²⁴ and $n_{\text{PBS}} = 1.33$.²⁵ The thicknesses of individual layers in the film were measured prior to deposition of subsequent layers. Hence, the thicknesses of the silicon oxide and polystyrene layers were accounted independently from thickness values measured for the Matrigel. When the thickness of Matrigel was measured, PBS was continuously flowed at 8 ml/min over the substrate so as to keep the system hydrated, and details of the flow chamber used are described elsewhere.²⁵ It was necessary to keep the Matrigel hydrated during ellipsometry, as it had been observed that upon exposure to air, Matrigel thin films dried out and contracted within minutes. Three surfaces were prepared and measured for each substrate type (i.e., SiO₂, polystyrene, and oxygen plasma treated polystyrene).

4. Scanning electron microscopy

Samples were imaged with a Hitachi S-5000 scanning electron microscope with an acceleration voltage of 10 kV. A drop of KO-DMEM diluted Matrigel sufficient to cover the entire surface was deposited on appropriately treated wafers (i.e., SiO₂ no treatment, polystyrene coating, polystyrene coating and subsequent oxygen plasma treatment). Samples were left to gel for 30 min and then tilted to allow excess fluid above the Matrigel layer to slide off. The fluid was wicked off by a kimwipe. The Matrigel samples were then fixed in 2% glutaraldehyde in 0.1M sodium cacodylate buffer, pH 7.2 for 2 h. They were rinsed three times in 0.1M sodium cacodylate buffer, pH 7.2 for 15 min each rinse. Samples were then dehydrated in graded ethanol to 100%. Samples were critical point dried, mounted onto stubs, dried overnight, then sputter coated with gold prior to imaging.

C. Cell culture

1. hES cell culturing

Human embryonic stem cells (HSF-6, University of California at San Francisco, and H9 lines, Wicell, Madison, WI)

were maintained on hES cell qualified Matrigel™ coated TCPS dishes in X-Vivo 10 medium (Lonza, Switzerland) supplemented with 80 ng/ml basic fibroblast growth factor (FGF-2, R&D Systems, Minneapolis MN) and 0.5 ng/ml transforming growth factor-beta1 (TGF- β 1, R&D Systems). This medium has previously been found to support hES cell self-renewal over extended periods of time.²⁶ Cells were passaged with 200 U/ml collagenase IV (Invitrogen) and seeded at 100 000 cells/cm² on Matrigel-coated TCPS, polystyrene, and glass. The medium was exchanged everyday on the samples.

2. Cell attachment and proliferation studies

For attachment and proliferation studies, cells were seeded at 100 000 cells/cm² and grown on Matrigel-coated TCPS, glass, or polystyrene (PS) for either 3 h to assess attachment or 5 days for proliferation. Attachment studies were also performed at the same initial cell seeding densities on uncoated TCPS, glass, and PS surfaces. All coated and uncoated surfaces were washed once with PBS after the 3 h incubation to remove unattached cells. Cell numbers for both studies were quantified with the Cyquant cell proliferation kit (Invitrogen). Statistical significant differences were determined using ANOVA between samples with a Tukey–Kramer *post hoc* test with $p < 0.05$. Statistics were only computed for samples of the same cell line.

3. Immunocytochemistry for Oct-4 and SSEA-4

On the fifth day after seeding, immunocytochemistry was performed on the samples for the POU family transcription factor OCT-4 and for the cell surface marker SSEA-4, which are both highly specific and necessary markers for undifferentiated hES cells. Cells were fixed in 4% paraformaldehyde and then permeabilized with 0.1% Triton X-100. The cells were incubated with 0.5% sodium dodecyl sulfate (SDS), blocked with 2% bovine serum albumin (BSA), and first incubated with the rabbit Oct-4 antibody (Abcam, Cambridge, MA) or SSEA-4 antibody (Millipore, Billerica, MA) overnight and then incubated with antirabbit Alexa 546 or anti-mouse Alexa 488 secondary antibodies (Invitrogen). 4',6-diamidino-2-phenylindole (DAPI) (Invitrogen) was added to the cells and then the cells were imaged.

4. Quantification of Oct-4 and SSEA-4 expression with flow cytometry

Oct-4 and SSEA-4 expressions were quantified with flow cytometry (Cytomics FC 500, Beckmann Coulter). For flow cytometry, cells were seeded and grown on Matrigel-coated TCPS, glass, or PS surfaces for 5 days. Cells were incubated with 2 mM ethylenediaminetetraacetic acid (EDTA) in PBS for 10–15 min to dissociate cells into single cells.

Cells to be examined for Oct-4 expression were first fixed in 2% formaldehyde in PBS for 20 min and washed with 2% fetal bovine serum (FBS) (Invitrogen) in PBS twice. Cells were then permeabilized with 1 mg/ml saponin (Fluka, St. Louis, MO) in 10% bovine serum albumin dissolved in PBS (SPB) for 15 min, and then incubated with Oct-4 antibody

(Abcam) for 1 h. Cells were washed with SPB then incubated with antirabbit Alexa 488 antibody (Invitrogen) for 1 h. Cells were then washed with SPB and then resuspended in 2% fetal bovine serum in PBS for analysis in a flow cytometer.

Cells to be examined for SSEA-4 were incubated with SSEA-4 antibody (Millipore) for 30 min, immediately after the EDTA cell dissociation described above. Cells were washed in 2% FBS in PBS twice and then incubated with antimouse Alexa 488 (Invitrogen) for 30 min. Cells were then washed twice in 2% FBS in PBS and then resuspended in 2% FBS in PBS for analysis in a flow cytometer. Statistical significant differences for Oct-4 and SSEA-4 expression were determined using ANOVA between samples with a Tukey–Kramer *post hoc* test with $p < 0.05$. Statistics were only computed for samples of the same cell line.

III. RESULTS AND DISCUSSION

The initial attachment and growth of hES cells on Matrigel was influenced by the underlying substrate (Fig. 1). In comparison to TCPS surfaces coated with Matrigel, glass and PS surfaces coated with Matrigel exhibited less initial cell attachment [Fig. 1(b)]. For the HSF-6 cell line, we found that ~30% of the cells attached to the Matrigel-coated TCPS surface, while glass and PS surfaces had 15% and 20% of the cells attached after 3 h, respectively. The H9 cells showed the same trend; however, for each surface less H9 cells attached compared to the HSF-6 cells (20% attachment on Matrigel-coated TCPS, 10% on Matrigel-coated PS, and 5% on Matrigel-coated glass). There was no detectable cell attachment on any substrate when Matrigel was absent from the surface. Since our culture medium was serum-free and did not contain serum-derived products, there were no proteins in the media that could adsorb and promote cell attachment. The phase images of the two cell lines (HSF-6 and H9) grown on Matrigel adsorbed onto PS, glass, and TCPS [Fig. 1(a)] and cell growth data [comparison of Figs. 1(b) and 1(c)] indicate that cells proliferated on Matrigel adsorbed onto hydrophilic surfaces (glass and TCPS), with the highest proliferation rates observed on TCPS. Matrigel adsorbed onto the hydrophobic surface, polystyrene, showed the greatest level of cell detachment during media exchange [comparison of Figs. 1(b) and 1(c)], rendering polystyrene a poor substrate for hES cell culturing. Additionally, Matrigel adsorbed onto PS and glass had a higher percentage of differentiated cells than Matrigel adsorbed onto TCPS, as can be seen by the increased presence of nonspherical cells in the phase images and in the low percentage of cells expressing the pluripotency markers Oct-4, a nuclear marker, and SSEA-4, a cell surface marker (Fig. 2, and see Ref. 28 for supplementary Fig. 1).

To better understand the cell proliferation and differentiation observations, the adsorption and film properties of Matrigel on the varying substrates were characterized by ellipsometry, QCM-D, and SEM. Sessile drop contact angle measurements of the prepared surfaces were performed with water in air and results, demonstrating the similar hydrophi-

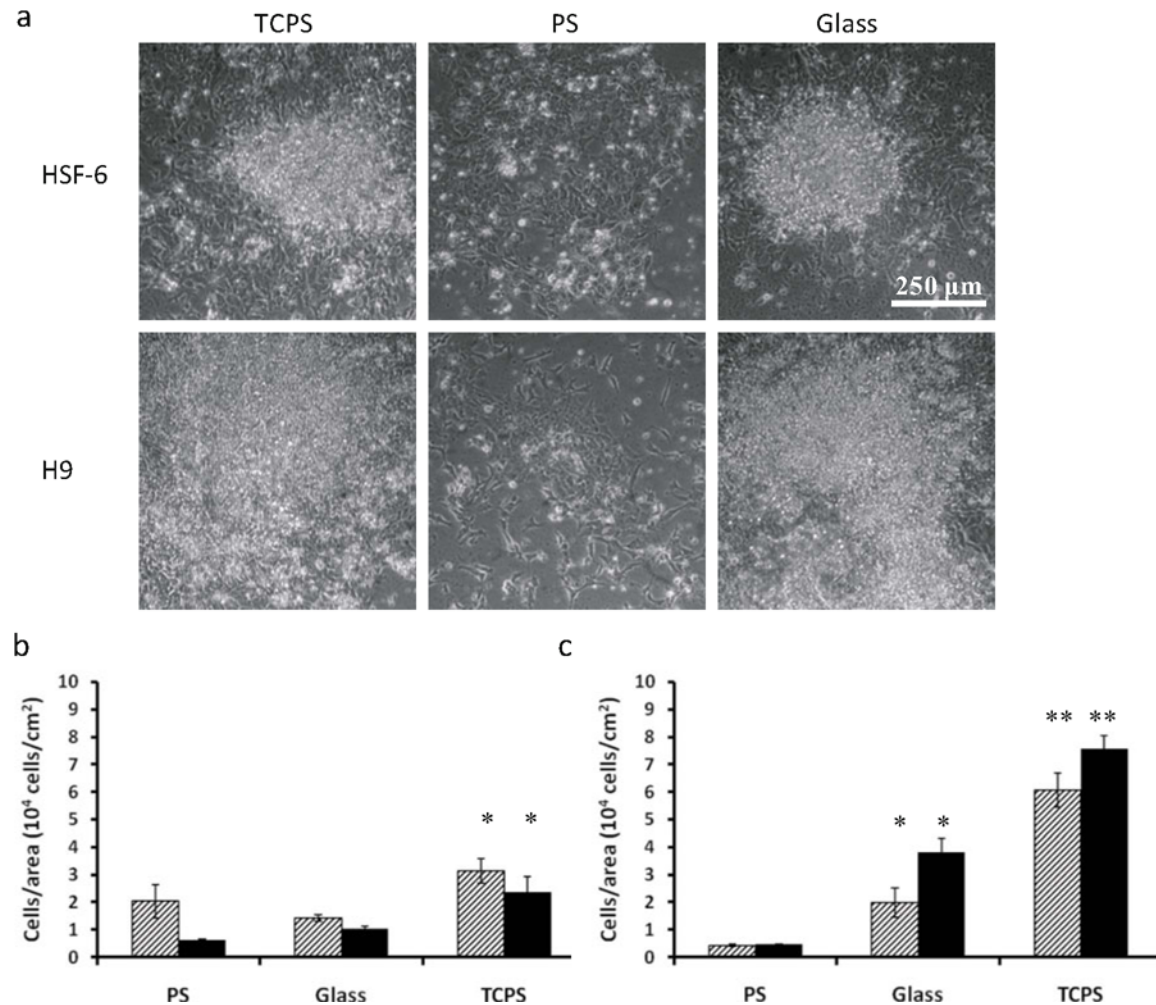


FIG. 1. (Color online) Phase images and proliferation of hES cells grown on the Matrigel-coated TCPS, PS, and glass. (a) After 5 days, both HSF-6 and H9 cells have colonies on TCPS indicated by closely packed cells. On PS, both cell lines differentiate to a larger extent as indicated by spread cells. On glass, both hES cell lines appear to have some colonies with morphology similar TCPS. Although these colonies do not have the typical hESC colony morphology seen with feeders, the exhibited morphology without colony borders is typical of some hESC lines on Matrigel (Refs. 6 and 27). (b) Attachment of hESCs to TCPS, PS, and glass surfaces coated with Matrigel. After 3 h, HSF-6 (▨) and H9 (■) cells attached on Matrigel-coated TCPS at higher levels than on the Matrigel-coated PS or glass. On surfaces without Matrigel, the amount of attached cells was below the detection level of the assay. Data represent mean \pm standard deviation. Values not in the same group (*) were statistically different from one another ($p < 0.05$ using ANOVA between groups with Tukey–Kramer significant difference *post hoc* test). (c) After 5 days, both hES cell lines HSF-6 (▨) and H9 (■) had significantly higher cell proliferation on the Matrigel-coated TCPS as compared to the Matrigel-coated glass or the Matrigel-coated PS. Values not in the same group (* or **) were statistically different from one another ($p < 0.05$ using ANOVA between groups with Tukey–Kramer significant difference *post hoc* test).

licity of oxygen plasma treated polystyrene and glass are reported in Table II. Adsorbed Matrigel displayed similar thicknesses on all three surfaces, with polystyrene showing the thickest Matrigel layer, and oxygen plasma treated polystyrene surfaces showing the greatest variability in Matrigel film thickness (Table III). The assumption, when modeling ellipsometry data, is that of flat homogeneous interfaces, and from SEM images [Figs. 3(a)–3(c)], it is evident that oxygen plasma treated polystyrene has a rougher surface than polystyrene or SiO₂, thus leading to the higher expected variability in Matrigel film thickness on that surface. The ellipsometry results also indicate that the ECM proteins in Matrigel form an adsorbed layer, approximately two orders of magnitude greater in thickness than a typical protein monolayer,²⁹ implying that the proteins form a multilayer, most likely an associative network or gel.

We sought to confirm the gel nature of the Matrigel films with QCM-D. If Matrigel behaved as a rigid thin elastic film (such as an idealized protein monolayer), the change in resonant frequency (Δf) of the quartz crystal upon Matrigel adsorption would be directly proportional to the change in mass, and the change in mass could be calculated from the Sauerbrey equation,

$$\Delta m = C\Delta f/n, \quad (1)$$

where m is the mass, f/n is the normalized resonant frequency overtone, and C is a constant which depends on the density, shear modulus, and transverse wave velocity in the crystal.³⁰ Figure 4 displays the frequency and dissipation re-

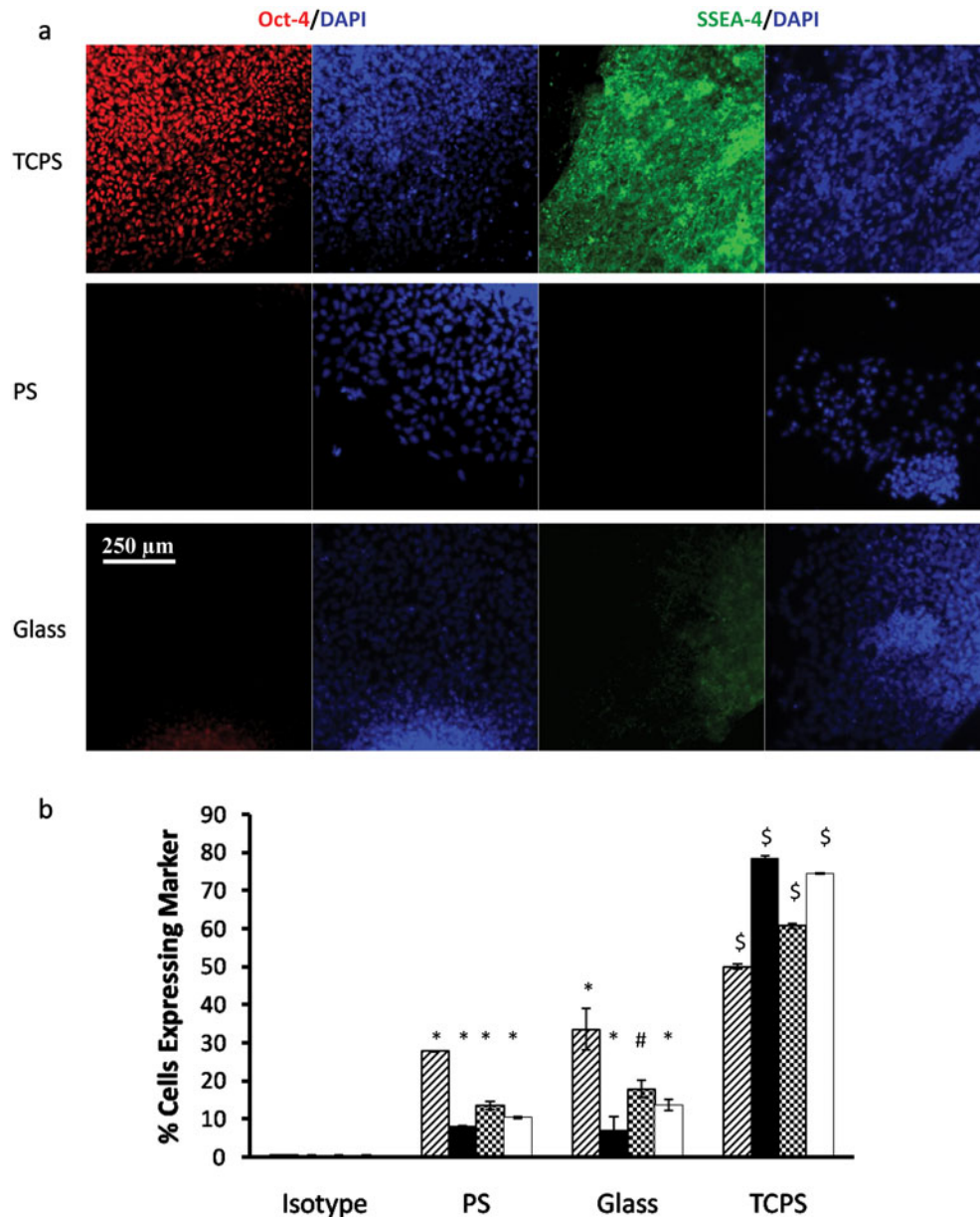


FIG. 2. (Color) Expression of the embryonic stem cell markers Oct-4 and SSEA-4 of hES cells grown on the Matrigel-coated TCPS, PS, and glass after 5 days. (a) Immunocytochemistry of Oct-4 and SSEA-4 on HSF-6 cells. (b) Quantification of SSEA-4 and Oct-4 via flow cytometry for cells cultured on Matrigel-coated surfaces, after 5 days of culture for H9 and HSF-6 cell lines. Matrigel-coated TCPS showed the largest percentage of cells expressing SSEA-4 for both hES cell lines H9 (▨) and HSF-6 (■), as compared to the Matrigel-coated PS and the Matrigel-coated glass which showed a lower, statistically similar amount of cells expressing SSEA-4. The Matrigel-coated TCPS also showed the largest percentage of cells expressing Oct-4 for both hES cell lines: H9 (▩) and HSF-6 (□). The H9 cell line showed significantly more Oct-4 expression on the Matrigel-coated glass than on the Matrigel-coated PS, but HSF-6 showed similar levels of expression on those two surfaces. Values not in the same group (*, #, or \$) were statistically different from one another ($p < 0.05$ using ANOVA between groups with Tukey–Kramer significant difference *post hoc* test). Only samples within the same cell line and for the same marker were compared statistically.

sponses of the functionalized (i.e., SiO₂, polystyrene, and oxygen plasma treated polystyrene) quartz crystals during the Matrigel adsorption experiment. Two features in those response curves indicate that Matrigel must be forming a gel on all three substrates. The first notable feature indicating that Matrigel is viscoelastic is the high dissipation (ΔD) of the film on all three surfaces. For monolayer protein films, which can be considered elastic, typical ΔD values are on the order of 1×10^{-6} .³¹ In contrast, ΔD was greater than 1.5×10^{-5} for Matrigel films on all surfaces (relative to the base

line of PBS on the crystal), and Matrigel on glass and oxygen plasma treated polystyrene surfaces showed ΔD values as high as 5×10^{-5} . Additionally, when a film is rigid and elastic, the normalized overtones will overlap; however, the normalized overtones do not overlap for any of the surfaces (Fig. 4). Therefore, on all of the surfaces tested, Matrigel forms an associative network or gel, and not a monolayer of mixed proteins.

For a viscoelastic film, such as Matrigel, the Voigt model can be used to describe the complex shear modulus such that

TABLE II. Sessile water-in-air contact angles of test surfaces.

Substrate	$\theta_{\text{H}_2\text{O}}$
Untreated glass slide, SiO ₂	28
SiO ₂ coated quartz crystal rinsed in water after toluene exposure	78
SiO ₂ coated quartz crystal immersed in water bath for 30 min after toluene exposure	26
SiO ₂ coated quartz crystal immersed in water bath over 24 h	14
SiO ₂ coated quartz crystal treated with O ₂ plasma	<10
Polystyrene coated quartz crystal	91
Oxygen plasma treated polystyrene coated quartz crystal	<10

$$G^* = G' + iG'' = \mu_f + i2\pi f \eta_f = \mu_f(1 + i2\pi f \tau), \quad (2)$$

where G' is the storage modulus and G'' is the loss modulus, μ_f is the elastic shear modulus (storage modulus) η_f is the shear viscosity, f is the oscillation frequency, and τ is the characteristic relaxation time of the film (which is proportional to the frequency and inversely proportional to the dissipation). Voinova *et al.*³² showed that when a viscoelastic film, under a semi-infinite bulk Newtonian liquid, has a shear acoustic wave applied to it (via elastic quartz below it), the change in resonant frequency and dissipation can be related to the film properties (thickness, density, elastic modulus, and viscosity) and to the bulk fluid properties (density and viscosity). However, since the viscosity and density of our Matrigel films are unknown, it was not possible to reliably

TABLE III. Adsorption properties of Matrigel™.

	Polystyrene ($n=3$)	SiO ₂ ($n=3$)	Oxygen plasma treated polystyrene ($n=3$)
Thickness (nm) ^a	453.6 ± 2.6	430.4 ± 1.6	432.9 ± 31.0
Maximum $\Delta F7/7$ ^b	-51.7 ± 3.3	-171 ± 1.0	-211.5 ± 0.8
Maximum $\Delta D7$ ^b	10.7 ± 0.4	44.1 ± 0.8	45.6 ± 0.7
Maximum $(\Delta F7/7)/(\Delta D7)$ ^b	4.82 ± 0.2	3.88 ± 0.1	4.64 ± 0.1

^aFrom ellipsometry.

^bAfter PBS wash.

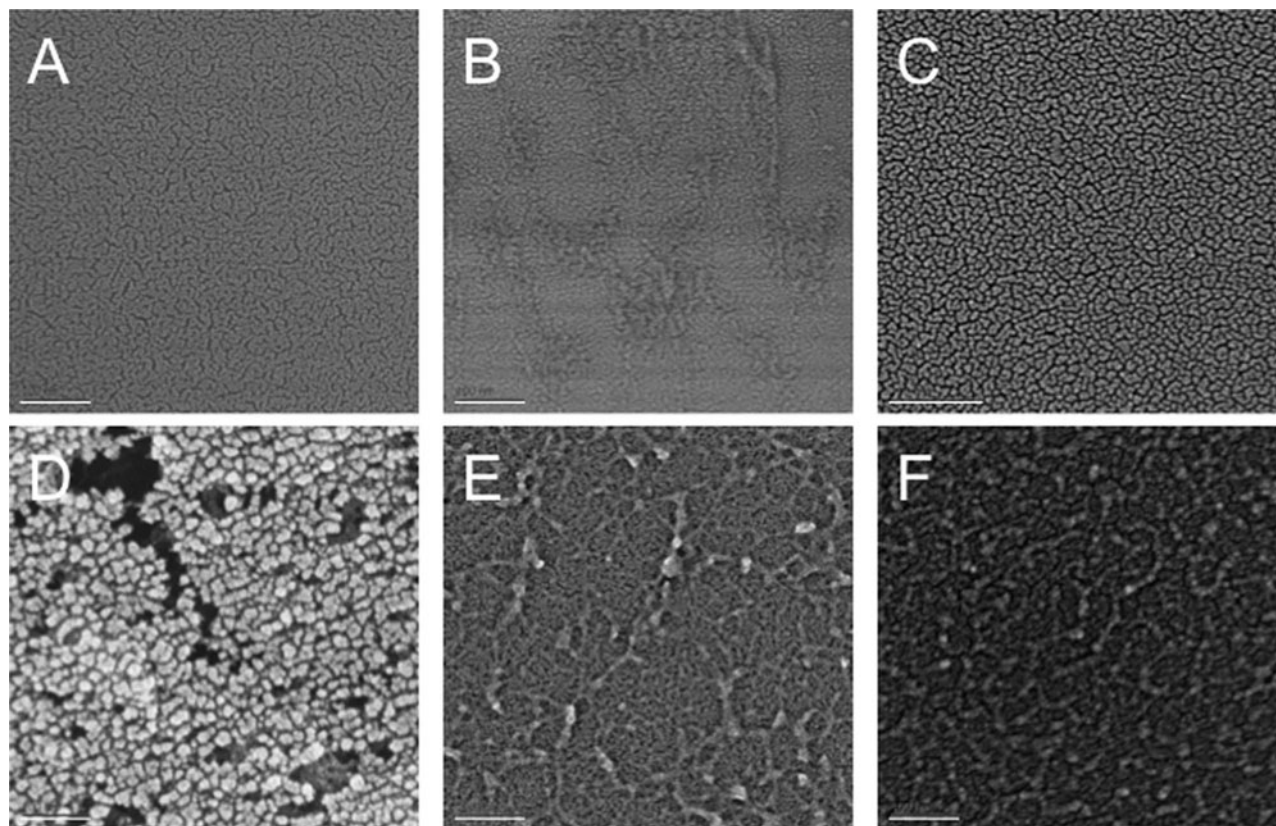


FIG. 3. SEM of bare substrates and substrates with Matrigel. Scale bar=100 nm. [(a)–(c)] Bare substrates: (a) is polystyrene, (b) is oxygen treated polystyrene, and (c) is glass. [(d)–(f)] Adsorbed Matrigel: (d) is Matrigel on polystyrene, (e) is Matrigel on oxygen plasma treated polystyrene, and (f) is Matrigel on glass.

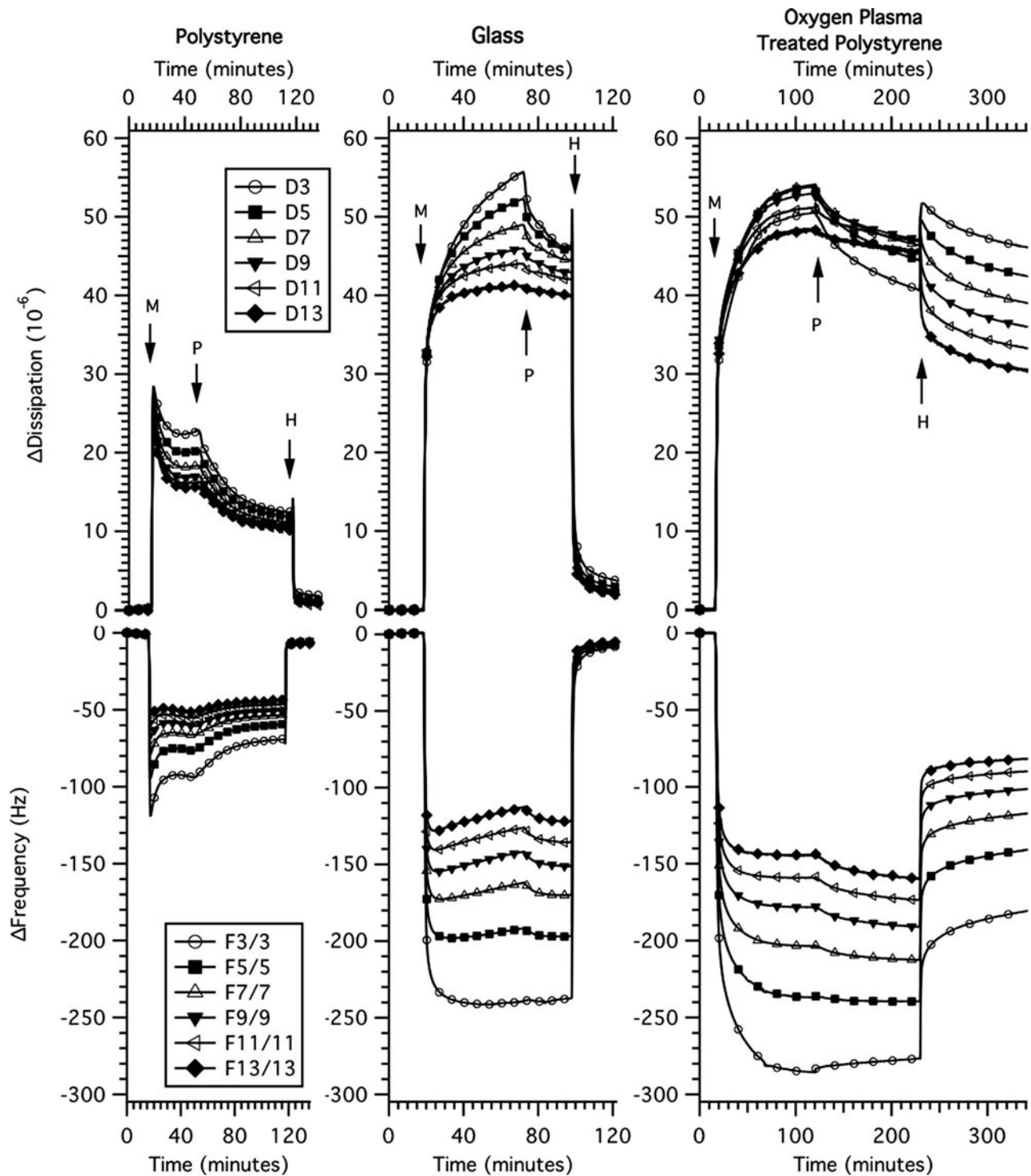


FIG. 4. Frequency and dissipation responses to the experimental procedure on all three surfaces probed. Base line frequency and dissipation were established with PBS flowing on the QCM-D crystal. Matrigel was then flowed over the quartz crystal until it saturated the surface. After maximum adsorption had been achieved, the crystal was rinsed with PBS. For the last step, the crystal was rinsed with the detergent Hellmanex. The arrows and letters indicate when each step occurred (*M* is Matrigel, *P* is PBS, and *H* is Hellmanex).

deduce thickness or modulus from the frequency and dissipation data from the QCM-D experiments. In fact, our SEM images demonstrate that the density of Matrigel is not identical on the three surfaces [Figs. 3(d)–3(f)]. Nevertheless, comparing information on the trends in frequency and dissipation

changes during the Matrigel adsorption experiment can still provide useful information.

One useful metric for comparing structural information from QCM-D data is the relationship $\Delta F/\Delta D$. We used the seventh overtone to show representative data and trends.

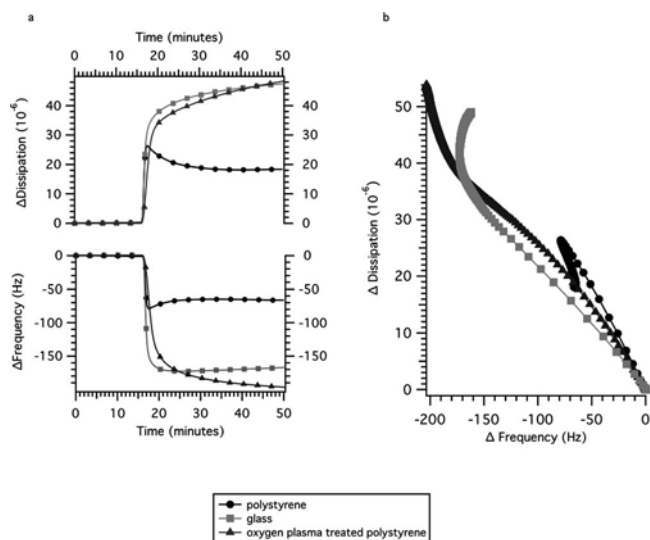


Fig. 5. Differences in kinetics of adsorption and conformation of Matrigel on the three surfaces are manifest in (a) the adsorption rates and (b) ΔF - ΔD plots for adsorption.

Matrigel adsorbed onto glass and onto oxygen plasma treated polystyrene had similar thicknesses as determined by ellipsometry and similar dissipation values at maximum adsorption (Table III). However, $\Delta F/\Delta D$ at maximum adsorption was different for the two surfaces, with the ratio $\Delta F/\Delta D$ larger for oxygen plasma treated polystyrene than for glass (Table III). Since thickness and dissipation were similar for the two surfaces, this indicates that either the elastic modulus, the viscosity, and/or the density differs for the two surfaces, supporting the notion that Matrigel has a different structure on glass than it does on oxygen plasma treated polystyrene, potentially leading to the varied cell behavior observed on those surfaces.

Examining the change in frequency and dissipation for the adsorption of Matrigel films on the varying substrates, it was observed that the kinetics of adsorption depended on the substrate [Fig. 5(a) and Table IV]. The kinetics of Matrigel adsorption were characterized by the time required to reach 75% of the maximum adsorption in the frequency curves (prior to any wash step). Matrigel adsorption was four times faster on glass than on oxygen plasma treated polystyrene surfaces. On polystyrene, a rapid initial adsorption was followed by an immediate desorption (prior to any rinse step) (Fig. 4) indicative of the weak and somewhat reversible bonds between Matrigel and the hydrophobic surface. Since the concentration of Matrigel flowed over each surface was

identical, we assumed that the effective diffusivity of proteins in Matrigel was the same for each experiment and that differences in time to maximum adsorption could therefore only reflect differences in either an initial affinity to the surface, surface restructuring based on conformation changes in the adsorbed proteins, or exchange reactions (i.e., the Vroman effect, in which proteins with a lower bulk concentration and a higher affinity for the surface will replace proteins with higher bulk concentration and lower surface affinity that reached the surface first).³³ If the initial affinity had been dominant in contributing to the differences in adsorption times, then we would expect the surface with the fastest adsorption time to have the strongest bonds with Matrigel. In fact, we saw the opposite phenomenon: The oxygen plasma treated polystyrene, which demonstrated the slowest adsorption kinetics, displayed the highest resistance to the Hellmanex (surfactant) rinse.

To assess whether the adsorption event contained structural changes in the protein network, ΔF - ΔD plots were constructed, where a change in slope would indicate a change in structuring, or potentially a Vroman effect behavior.³¹ The simplest ΔF - ΔD plot for protein monolayer adsorption exhibits a linear relationship. None of the surfaces examined showed a linear relationship for the entire adsorption range [Fig. 5(b)]. Both polystyrene and glass exhibited an initial linear region (at low frequency and low dissipation) followed by a nonmonotonic region. For polystyrene this feature may indicate either an initial desorption (both frequency and dissipation decrease right after adsorption) or a conformational change in the ECM proteins, where the proteins unfold to expose hydrophobic regions to dehydrate the interface and minimize interfacial free energy. Oxygen plasma treated polystyrene exhibits linearity only at very low frequency/dissipation values and then at high frequency/high dissipation. Even though glass and oxygen treated polystyrene are hydrophilic surfaces, the differences in adsorption rate and ΔF - ΔD plots indicate that they structure Matrigel in a different manner.

We also observed that the surfaces had different responses to elution buffers. On the polystyrene surface, the PBS wash decreased both the magnitude of the frequency and dissipation responses (ΔF and ΔD), while on the hydrophilic surfaces (glass and oxygen plasma treated polystyrene) the magnitude of the frequency increased while the magnitude of the dissipation decreased (Fig. 4). It is likely that the PBS removed loosely adhered proteins on the polystyrene, hence a decrease in both parameters. It is less clear how the PBS rinse affected the hydrophilic Matrigel-coated surfaces; how-

TABLE IV. Kinetics of Matrigel™ adsorption and effect of rinsing on network stability.

	Polystyrene ($n=3$)	SiO ₂ ($n=3$)	Oxygen plasma treated polystyrene ($n=3$)
Time to 75% adsorption (s)	^a	62.0 ± 0.1	255.7 ± 8.3
Hellmanex rinse final $\Delta F/7$	-4.2 ± 1.8 (8.1%)	-4.1 ± 4.4 (2.4%)	-118.6 ± 2.4 (55.4%)
Hellmanex rinse final $\Delta D/7$	0.3 ± 0.5 (3.4%)	3.7 ± 1.9 (8.4%)	39.1 ± 0.6 (83.3%)

^aThe adsorption curve showed a rapid initial adsorption followed by an immediate desorption prior to any wash steps (see Fig. 2) rendering the time to 75% adsorption unclear for the polystyrene surface

ever, we believe that PBS controls the swelling of Matrigel on those surfaces. This interpretation of the data is supported by the SEM images (Fig. 3), which show that Matrigel on polystyrene forms a structure composed of globules, while Matrigel on hydrophilic surfaces forms a fibrillar network. When the Matrigel proteins deposit on polystyrene, they presumably change conformation to expose hydrophobic pockets and expel water. Ultimately, the associative gel composed of those proteins will have exposed hydrophobic areas and resist water uptake, yielding a more compressed and rigid structure in PBS (which can be seen in the low dissipation values). The hydrophilic surfaces (glass and oxygen plasma treated polystyrene) both have fibrillar structures reminiscent of protein hydrogels and large dissipation values implying that they are soft, which can be a consequence of associated water.³⁴ If adsorbed Matrigel acts a hydrogel, it is likely that PBS controls its swelling behavior.

The most pronounced difference between the hydrophilic surfaces was the response of Matrigel to the Hellmanex wash (Fig. 4). Hellmanex is composed of wetting agents, emulsifiers, ampholytic surfactants, complexing agents, and potassium phosphate. The ease with which Hellmanex can remove Matrigel from a surface can be indicative of the strength of the gel structure of Matrigel and/or the bonding strength between Matrigel and the underlying substrate. Hellmanex was able to remove nearly all the Matrigel on the polystyrene and glass surfaces (Fig. 4 and Table IV), as indicated by the frequency and dissipation reaching near base line values on those surfaces after the Hellmanex wash. In contrast, the oxygen plasma treated polystyrene showed a markedly smaller response to the Hellmanex wash, with 55.4% of the adsorption frequency and 83.3% of the adsorption dissipation remaining after the wash. The inability of the surfactant to remove most of the protein network on the oxygen plasma treated polystyrene surface leads us to believe that the interface and part of the gel structure involve strong nearly irreversible bonds. Considering that the Matrigel-substrate interfacial bond varies drastically with substrate type, we suggest that ECM proteins in Matrigel orient differently at the interface with each substrate, exposing different proteins and/or chemical moieties, depending on the topography and chemistry of the substrate, and that the initial protein deposition affects gel formation, ultimately leading to the varied cell behaviors observed. Ideally it would be informative to measure the composition of Matrigel adsorbed to each surface. However, this is an impossible task as Matrigel contains over a 1000 different proteins,³⁵ and therefore techniques do not exist to give a quantitative measurement of composition of the adsorbed proteins.

To determine how the underlying substrate affects the Matrigel-liquid interface (i.e., the surface which cells interrogate), scanning electron microscopy was performed on all three surfaces, both with and without Matrigel (Fig. 3). Polystyrene and glass surfaces were both smoother than oxygen treated polystyrene surfaces [Figs. 3(a)–3(c)]. It is possible that the differences in topography between oxygen plasma treated polystyrene and glass, in addition to the differences in

chemistry, affect Matrigel adsorption. On the polystyrene surface, Matrigel forms a porous structure made up of globular units. On both the glass surface and the oxygen plasma treated polystyrene, Matrigel is characterized by a fibrillar and less globular structure. Adsorbed ECM proteins may need to form a fibrillar network in order to support hES cell attachment, as cells attach readily on Matrigel that has been adsorbed onto either oxygen treated polystyrene or glass, but not onto Matrigel adsorbed onto untreated polystyrene. Even though both hydrophilic surfaces caused Matrigel to form a fibrillar structure, the Matrigel network that formed on SiO₂ was a morphologically distinct, denser network than the network that formed on oxygen treated polystyrene. We therefore conclude that the differences observed for cell proliferation and differentiation on Matrigel adsorbed onto the hydrophilic surfaces were due to differences in Matrigel structuring on each surface. As we have shown with QCM-D and SEM, the density and the mechanical properties of Matrigel were not identical on the two surfaces. The density of the structure affects cell fate by dictating the distance between chemical moieties and ligands, ultimately controlling internal cell signaling.^{36–40} Many studies have also demonstrated the link between the mechanical environment surrounding the cell (i.e., the extracellular matrix) and internal cell signaling,^{41–44} specifically linking the mechanical properties of the ECM with cell proliferation^{45,46} and differentiation.^{47–49} It is therefore, not surprising that differing structures of Matrigel on the examined substrates lead to differing cell fates.

IV. CONCLUSIONS

We found that human embryonic stem cells respond differently to Matrigel treated surfaces depending on the underlying substrate, and our findings may be exploited as design parameters for the development of artificial ECM systems for human embryonic stem cell culture. Hydrophobic substrates did not support the attachment and proliferation of human embryonic stem cells, and we correlated this observation with the Matrigel adsorption behavior. Additionally, we have shown that despite the similar wetting properties of glass and oxygen plasma treated polystyrene, Matrigel exhibits differing mechanical properties, film stability, and structure on those surfaces, ultimately leading to enhanced cell proliferation and maintenance of the pluripotent state on the Matrigel-coated oxygen plasma treated polystyrene relative to the Matrigel-coated glass.

ACKNOWLEDGMENTS

This work was supported in part by a Berkeley Futures Grant (KEH) (No. R01GM085754) and an Applied Biology and Bioprocess Engineering Training Grant (NIH Grant No. T32 GM08352). Ellipsometry was performed in Clay Radke's laboratory, University of California, Berkeley (Berkeley, CA, USA). Scanning electron microscopy was performed at the Electron Microscope Laboratory, University of California, Berkeley (Berkeley, CA, USA). Quartz Crystal Microbalance studies were performed in Gabor Somorjai's

laboratory, University of California, Berkeley (Berkeley, CA, USA). The authors would like to thank Sam Maurer, Guangwei Min, and George Holinga for their technical assistance with ellipsometry, scanning electron microscopy, and quartz crystal microbalance studies, respectively.

- ¹J. A. Thomson, J. Itskovitz-Eldor, S. S. Shapiro, M. A. Waknitz, J. J. Swiergiel, V. S. Marshall, and J. M. Jones, *Science* **282**, 1145 (1998).
- ²B. E. Reubinoff, M. F. Pera, C. Y. Fong, A. Trounson, and A. Bongso, *Nat. Biotechnol.* **18**, 399 (2000).
- ³J. M. Fletcher *et al.*, *Cloning Stem Cells* **8**, 319 (2006).
- ⁴M. Richards, C. Y. Fong, W. K. Chan, P. C. Wong, and A. Bongso, *Nat. Biotechnol.* **20**, 933 (2002).
- ⁵L. Z. Cheng, H. Hammond, Z. H. Ye, X. C. Zhan, and G. Dravid, *Stem Cells* **21**, 131 (2003).
- ⁶O. Genbacev *et al.*, *Fertil. Steril.* **83**, 1517 (2005).
- ⁷M. J. Martin, A. Muotri, F. Gage, and A. Varki, *Nat. Med.* **11**, 228 (2005).
- ⁸L. G. Chase and M. T. Firpo, *Curr. Opin. Chem. Biol.* **11**, 367 (2007).
- ⁹C. H. Xu, M. S. Inokuma, J. Denham, K. Golds, P. Kundu, J. D. Gold, and M. K. Carpenter, *Nat. Biotechnol.* **19**, 971 (2001).
- ¹⁰Y. Li, S. Powell, E. Brunette, J. Lebkowski, and R. Mandalam, *Biotechnol. Bioeng.* **91**, 688 (2005).
- ¹¹S. Yao, S. Chen, J. Clark, E. Hao, G. M. Beattie, A. Hayek, and S. Ding, *Proc. Natl. Acad. Sci. U.S.A.* **103**, 6907 (2006).
- ¹²G. M. Beattie, A. D. Lopez, N. Bucay, A. Hinton, M. T. Firpo, C. C. King, and A. Hayek, *Stem Cells* **23**, 489 (2005).
- ¹³T. E. Ludwig *et al.*, *Nat. Biotechnol.* **24**, 185 (2006).
- ¹⁴B. D. Biosciences, see: <http://viewer.zmags.com/publication/d5d7952b?page=124>.
- ¹⁵H. K. Kleinman, M. L. McGarvey, L. A. Liotta, P. G. Robey, K. Tryggvason, and G. R. Martin, *Biochemistry* **21**, 6188 (1982).
- ¹⁶S. L. Barker and P. J. Larocca, *J. Tissue Cult. Methods* **16**, 151 (1994).
- ¹⁷A. S. G. Curtis, J. V. Forrester, C. McInnes, and F. Lawrie, *J. Cell Biol.* **97**, 1500 (1983).
- ¹⁸T. Englander, D. Wiegel, L. Naji, and K. Arnold, *J. Colloid Interface Sci.* **179**, 635 (1996).
- ¹⁹M. Fletcher and K. C. Marshall, *Appl. Environ. Microbiol.* **44**, 184 (1982).
- ²⁰E. F. Irwin, J. E. Ho, S. R. Kane, and K. E. Healy, *Langmuir* **21**, 5529 (2005).
- ²¹J. C. Munro and C. W. Frank, *Macromolecules* **37**, 925 (2004).
- ²²L. L. Foose, H. W. Blanch, and C. J. Radke, *J. Biotechnol.* **132**, 32 (2007).
- ²³J. Brandrup and E. H. Immergut, *Polymer Handbook*, 2nd ed. (Wiley, New York, 1975).
- ²⁴N. A. Lockwood, J. C. Mohr, L. Ji, C. J. Murphy, S. R. Palecek, J. J. de Pablo, and N. L. Abbott, *Adv. Funct. Mater.* **16**, 618 (2006).
- ²⁵L. L. Foose, H. W. Blanch, and C. J. Radke, *Langmuir* **24**, 7388 (2008).
- ²⁶Y. W. Zhang, J. Denham, and R. S. Thies, *Stem Cells Dev.* **15**, 943 (2006).
- ²⁷C. H. Xu *et al.*, *Stem Cells* **23**, 315 (2005).
- ²⁸See EPAPS supplementary material at E-BJIOBN-4-003904 for immunocytochemistry for the H9 cell line (Oct-4 and SSEA-4 staining on Matrigel coated onto all of the test surfaces). For more information on EPAPS, see <http://www.aip.org/pubservs/epaps.html>.
- ²⁹S. Balamurugan, L. K. Ista, J. Yan, G. P. López, J. Fick, M. Himmelhaus, and M. Grunze, *J. Am. Chem. Soc.* **127**, 14548 (2005).
- ³⁰G. Sauerbrey, *Z. Phys.* **155**, 206 (1959).
- ³¹F. Höök, M. Rodahl, B. Kasemo, and P. Brzezinski, *Proc. Natl. Acad. Sci. U.S.A.* **95**, 12271 (1998).
- ³²M. V. Voinova, M. Rodahl, M. Jonson, and B. Kasemo, *Phys. Scr.* **59**, 391 (1999).
- ³³F. Fang, J. Satulovsky, and I. Szleifer, *Biophys. J.* **89**, 1516 (2005).
- ³⁴F. Höök, B. Kasemo, T. Nylander, C. Fant, K. Sott, and H. Elwing, *Anal. Chem.* **73**, 5796 (2001).
- ³⁵K. C. Hansen, L. Kiemele, O. Maller, J. O'Brien, A. Shankar, J. Fornetti, and P. Schedin, *Mol. Cell Proteomics* **8**, 1648 (2009).
- ³⁶R. McBeath, D. M. Pirone, C. M. Nelson, K. Bhadriraju, and C. S. Chen, *Dev. Cell* **6**, 483 (2004).
- ³⁷K. Bhadriraju, M. Yang, S. A. Ruiz, D. Pirone, J. Tan, and C. S. Chen, *Exp. Cell Res.* **313**, 3616 (2007).
- ³⁸G. Maheshwari, G. Brown, D. A. Lauffenburger, A. Wells, and L. G. Griffith, *J. Cell Sci.* **113**, 1677 (2000).
- ³⁹D. L. Elbert and J. A. Hubbell, *Biomacromolecules* **2**, 430 (2001).
- ⁴⁰M. Arnold, E. A. Cavalcanti-Adam, R. Glass, J. Blümmel, W. Eck, M. Kanteleiner, H. Kessler, and J. P. Spatz, *ChemPhysChem* **5**, 383 (2004).
- ⁴¹D. E. Discher, P. Janmey, and Y. L. Wang, *Science* **310**, 1139 (2005).
- ⁴²L. A. Flanagan, Y. E. Ju, B. Marg M. Osterfield, and P. A. Janmey, *NeuroReport* **13**, 2411 (2002).
- ⁴³R. J. Pelham and Y. L. Wang, *Proc. Natl. Acad. Sci. U.S.A.* **94**, 13661 (1997).
- ⁴⁴M. J. Paszek *et al.*, *Cancer Cells* **8**, 241 (2005).
- ⁴⁵D. P. McDaniel, G. A. Shaw, J. T. Elliott, K. Bhadriraju, C. Meuse, K. H. Chung, and A. Plant, *Biophys. J.* **92**, 1759 (2007).
- ⁴⁶M. T. Thompson, M. C. Berg, I. S. Tobias, M. F. Rubner, and K. J. Van Vliet, *Biomaterials* **26**, 6836 (2005).
- ⁴⁷T. Boonthekul, E. E. Hill, H. J. Kong, and D. J. Mooney, *Tissue Eng.* **13**, 1431 (2007).
- ⁴⁸A. Engler, L. Bacakova, C. Newman, A. Hategan, M. Griffin, and D. Discher, *Biophys. J.* **86**, 617 (2004).
- ⁴⁹S. R. Peyton, C. B. Raub, V. P. Keschrumrus, and A. J. Putnam, *Biomaterials* **27**, 4881 (2006).